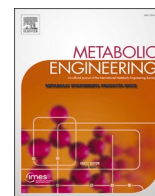




Contents lists available at ScienceDirect

## Metabolic Engineering

journal homepage: [www.elsevier.com/locate/meteng](http://www.elsevier.com/locate/meteng)

# Biosensor-informed engineering of *Cupriavidus necator* H16 for autotrophic D-mannitol production

Erik K.R. Hanko<sup>a,b</sup>, Gillian Sherlock<sup>a</sup>, Nigel P. Minton<sup>a</sup>, Naglis Malys<sup>a,\*</sup>

<sup>a</sup> BBSRC/EPSRC Synthetic Biology Research Centre (SBRC), School of Life Sciences, The University of Nottingham, Nottingham, NG7 2RD, United Kingdom

<sup>b</sup> Present address: Manchester Centre for Fine and Speciality Chemicals (SYNBIOCHEM), Manchester Institute of Biotechnology, University of Manchester, Manchester, M1 7DN, United Kingdom

## ARTICLE INFO

## Keywords:

*C. necator* H16  
Calvin cycle  
Mannitol  
Autotrophic fermentation  
Biosensor

## ABSTRACT

*Cupriavidus necator* H16 is one of the most researched carbon dioxide (CO<sub>2</sub>)-fixing bacteria. It can store carbon in form of the polymer polyhydroxybutyrate and generate energy by aerobic hydrogen oxidation under lithoautotrophic conditions, making *C. necator* an ideal chassis for the biological production of value-added compounds from waste gases. Despite its immense potential, however, the experimental evidence of *C. necator* utilisation for autotrophic biosynthesis of chemicals is limited. Here, we genetically engineered *C. necator* for the high-level *de novo* biosynthesis of the industrially relevant sugar alcohol mannitol directly from Calvin-Benson-Bassham (CBB) cycle intermediates. To identify optimal mannitol production conditions in *C. necator*, a mannitol-responsive biosensor was applied for screening of mono- and bifunctional mannitol 1-phosphate dehydrogenases (MtdDs) and mannitol 1-phosphate phosphatases (MIPs). We found that MtdD/MIP from brown alga *Ectocarpus siliculosus* performed overall the best under heterotrophic growth conditions and was selected to be chromosomally integrated. Consequently, autotrophic fermentation of recombinant *C. necator* yielded up to 3.9 g/L mannitol, representing a substantial improvement over mannitol biosynthesis using recombinant cyanobacteria. Importantly, we demonstrate that at the onset of stationary growth phase nearly 100% of carbon can be directed from the CBB cycle into mannitol through the glyceraldehyde 3-phosphate and fructose 6-phosphate intermediates. This study highlights for the first time the potential of *C. necator* to generate sugar alcohols from CO<sub>2</sub> utilising precursors derived from the CBB cycle.

## 1. Introduction

The production of chemicals and fuels from renewable biological resources or waste forms a rapidly growing segment of the bioeconomy. In the past decade, considerable progress has been made towards developing microbial cell factories for the conversion of waste gases, such as carbon dioxide (CO<sub>2</sub>), into value-added compounds (Yunus et al., 2018; Grenz et al., 2019; Panich et al., 2021; Jiang et al., 2021). CO<sub>2</sub> is produced during a wide range of natural and industrial processes and acts as a key greenhouse gas responsible for global climate change. One of the UN sustainable development goals is a transition towards net-zero carbon emissions by 2050 (Pavez et al., 2018), for which the utilisation of CO<sub>2</sub> as an abundant and low-cost feedstock for the synthesis of chemicals and fuels is hugely beneficial. However, considering the enormous amount of basic and applied research that has been carried out to produce value-added chemicals and fuels in the last few

decades, there is only a limited number of examples where thermodynamically stable and highly inert CO<sub>2</sub> is utilised as a feedstock in industrially sustainable processes. The large scale transformation of CO<sub>2</sub> into valuable products through heterogeneous catalysis requires a significant input of energy and is primarily based on the use of high-energy hydrogen and methane, yielding only a few compounds that are industrially sustainable to produce at large scale, including methane, higher hydrocarbons (Fischer-Tropsch synthesis), methanol, formic acid, and dimethyl ether (Kondratenko et al., 2013; Ye et al., 2019; Ra et al., 2020; Kamkeng et al., 2021). Photo- and electrocatalysis show potential for use in the conversion of CO<sub>2</sub> into chemicals and fuels, building on recent technical and catalytic advances that enable improved energy efficiency and productivity (Bushuyev et al., 2018; Ješić et al., 2021), whereas biocatalysis or microbial cell factory-based technologies require further development to become economically viable.

Chemolithoautotrophic *Cupriavidus necator* (formerly known as

\* Corresponding author.

E-mail address: [n.malys@gmail.com](mailto:n.malys@gmail.com) (N. Malys).

<https://doi.org/10.1016/j.ymben.2022.02.003>

Received 27 November 2021; Received in revised form 7 February 2022; Accepted 7 February 2022

Available online 8 February 2022

1096-7176/© 2022 The Authors. Published by Elsevier Inc. on behalf of International Metabolic Engineering Society. This is an open access article under the CC BY license (<http://creativecommons.org/licenses/by/4.0/>).

*Ralstonia eutropha*) is capable of fixing CO<sub>2</sub> through a reductive pentose phosphate cycle, i.e. CBB cycle. In the absence of organic substrates, it can utilise CO<sub>2</sub> and H<sub>2</sub> as sole carbon and energy sources. Due to its ability to store large amounts of reduced carbon in the form of polyhydroxybutyrate (PHB) (Schlegel et al., 1961a; Steinbüchel and Schlegel, 1991), *C. necator* is considered a promising host organism for the sustainable production of value-added compounds from CO<sub>2</sub>. In the last decade, with an extensive genetic toolkit available, allowing genome editing and the controlled expression of heterologous genes, *C. necator* has been engineered for the autotrophic production of methyl ketones (Müller et al., 2013), alka(e)nes (Crépin et al., 2016), isopropanol (Marc et al., 2017), α-humulene (Krieg et al., 2018), acetoin (Windhorst and Gescher, 2019), trehalose (Löwe et al., 2021), lipochitooligosaccharides (Nangle et al., 2020), 2,3-butanediol (Bommareddy et al., 2020) and 1, 3-butanediol (Gascoyne et al., 2021). A majority of these compounds are biosynthesised utilising precursors such as pyruvate and acetyl-CoA derived from the Entner–Doudoroff (ED) pathway.

Under autotrophic growth conditions, hexoses or their derivatives can be directly synthesised from CO<sub>2</sub> and water via the Calvin-Benson-Bassham (CBB) pathway with the energy (ATP) and reducing power (NADH), required for carbon fixation, generated by membrane-bound and soluble hydrogenases (Nybo et al., 2015). D-Mannitol (hereafter denoted mannitol) is an acyclic hexose alcohol that is naturally present in many plant species and can be synthesised by a wide range of microorganisms including bacteria, yeasts, fungi, lichens, and algae (Wiselink et al., 2002). For example, the brown alga *Laminaria digitata* (also commonly known as oarweed) accumulates mannitol as carbon and energy source up to 20% of its dry weight (Schiener et al., 2015). Mannitol is widely utilised in the food, pharmaceutical, chemical, and medical industries. As a food additive with a glycemic index of zero, it has no significant effects on blood sugar levels and is therefore used as a low-caloric sweetener suitable for diabetics (Song and Vieille, 2009). In medicine, mannitol is routinely employed as a diuretic and dehydrating agent administered to treat edema, hydrocephalus and glaucoma (Dai et al., 2017). Moreover, due to its low hygroscopicity, chemical stability and sweet cool taste, which may mask the unpleasant taste of drugs, mannitol is often used in the manufacture of chewing gum, tablets and granulated powders (Patra et al., 2009).

Mannitol can be obtained by extraction, chemical synthesis, and biosynthesis. Extraction of mannitol from plants using supercritical CO<sub>2</sub> or pressurised hot water has been successfully demonstrated (Ghoreishi and Sharifi, 2001; Ghoreishi and Shahrestani, 2009). Its application, however, is limited by the availability of raw material and seasonal variation in mannitol content (Schiener et al., 2015). Currently, mannitol is produced industrially by catalytic hydrogenation of fructose/glucose mixtures with sorbitol as a byproduct (Wisnlak and Simon, 1979). Although significant progress has been made towards developing catalysts with higher selectivity to mannitol (Zelin et al., 2019), separation from its isomer sorbitol and chromatographic removal of the metal catalyst remain challenging. The biological production of mannitol is mainly achieved by fermentation of lactic acid bacteria *Lactobacillus intermedius* and yeast *Candida magnoliae* using fructose and glucose as carbon sources resulting in high mannitol titres (>100 g/L), productivities (>4 g/L/h) and yields (>0.5 [(C-mol mannitol)/(C-mol hexose)]) (Racine and Saha, 2007; Savergave et al., 2013). Besides, similarly high titres, productivities and yields have been achieved through whole-cell biotransformation of glucose and fructose using recombinant *Escherichia coli* and *Corynebacterium glutamicum*, respectively (Kaup et al., 2005; Bäumchen and Bringer-Meyer, 2007).

In this study, we used *C. necator* H16 as a microbial chassis and as a whole cell biosensor to evaluate monofunctional mannitol 1-phosphate dehydrogenases (MtlDs) and mannitol 1-phosphate phosphatases (M1Ps), as well as bifunctional MtlD/M1Ps originating from several kingdoms of life for mannitol biosynthesis. A mannitol biosensor was applied not only to screen the combination of genes that enables the highest production of mannitol, but also to identify optimal conditions

for gene expression induction. For stable production of mannitol, *C. necator* was engineered by integration of mannitol biosynthesis genes into two different genomic loci, including PHB biosynthesis inactivation. The autotrophic production of mannitol using CO<sub>2</sub> as sole carbon source was demonstrated in batch fermentations yielding mannitol titres, productivities and yields that are substantially higher than previously reported for other CO<sub>2</sub>-fixing bacteria. This work highlights the potential of *C. necator* to be used as chassis organism for the economically viable conversion of CO<sub>2</sub> into sugar alcohols.

## 2. Materials and methods

### 2.1. Base strains and media

*E. coli* DH5α (New England BioLabs, NEB) was employed for cloning and plasmid propagation. *E. coli* S17-1 λpir was used as conjugation donor. *C. necator* H16 was used for heterologous expression of mannitol biosynthetic genes. All bacterial strains used in this study are listed in Table 1. Both *E. coli* and *C. necator* were routinely grown in lysogeny broth (LB) (Sambrook and Russell, 2001). Low-salt LB (LSLB)-MOPS was used for conjugative plasmid transfer and gene replacement (Lenz et al., 1994). The initial screening of genes for mannitol biosynthesis in *C. necator* and the heterotrophic production of mannitol in small volumes were performed in chemically defined minimal medium (MM) (Schlegel et al., 1961b) supplemented with 1 mL/L trace element solution SL7 (Trüper and Pfennig, 1981) and 0.4% (w/v) sodium-gluconate as carbon source. The mannitol biosensor-assisted investigation of inducer range and the heterotrophic production of mannitol in shake flasks were performed in LB medium. Pre-cultures for bioreactor cultivations were set up in Hanahan's broth (SOB medium) (Hanahan, 1983). Autotrophic production of mannitol was performed in modified DSMZ 81 medium (Bommareddy et al., 2020). When appropriate, the medium was supplemented with the following antibiotics: tetracycline (12.5 µg/mL for *E. coli* or 15 µg/mL *C. necator*), chloramphenicol (25 µg/mL for *E. coli* or 50 µg/mL *C. necator*), or gentamycin (10 µg/mL). For solid media preparation, 15 g/L agar was added. All chemicals, including media components, were purchased from Sigma-Aldrich unless indicated otherwise.

### 2.2. Cloning and transformation

Plasmid DNA was extracted using the QIAprep Spin Miniprep Kit (Qiagen). Bacterial genomic DNA was isolated using the GenElute Bacterial Genomic DNA Kit (Sigma-Aldrich). Oligonucleotide primers were synthesised by Sigma-Aldrich and are listed in Supplementary Table 1. DNA for cloning was amplified by PCR in 50 µL reactions using Phusion High-Fidelity DNA polymerase (NEB). Screening of bacterial colonies for successful assembly of vectors was performed using DreamTaq Green

**Table 1**  
Strains used and generated in this study.

Strain	Parental strain	Genotype/description	Reference or source
<i>E. coli</i> DH5α	–	<i>fhuA2 (argF-lacZ)U169 phoA glnV44 80 (lacZ)M15 gyrA96 recA1 relA1 endA1 thi-1 hsdR17</i>	NEB
S17-1 λpir	–	<i>thi pro hsdR hsdM<sup>+</sup> recA RP4-2-Tc::Mu-Km::Tn7 λpir T<sup>R</sup> Sm<sup>R</sup></i>	Simon et al. (1983)
<i>C. necator</i> H16	–	Wild type strain (DSM 428)	DSMZ
NM0010	H16	<i>ΔphaCAB, P<sub>araC</sub>-araC, P<sub>araBAD</sub>-mtlD/m1p<sup>a</sup></i>	This study
NM0011	H16	<i>ΔtcuAB, P<sub>araC</sub>-araC, P<sub>araBAD</sub>-mtlD/m1p<sup>a</sup></i>	This study
NM0013	H16	<i>ΔphaCAB, P<sub>phaC</sub>-mtlD/m1p<sup>a</sup></i>	This study

<sup>a</sup> *mtlD/m1p*: N-terminal truncated version of MtlD and M1P2 from *E. siliculosus*.

PCR Master Mix (2X, Thermo Fisher Scientific) in 25  $\mu$ L reactions. Gel-purified linearised DNA was extracted using the Zymoclean Gel DNA Recovery Kit. Restriction enzymes, T4 DNA ligase and the NEBuilder HiFi DNA Assembly Master Mix were purchased from NEB. PCR-, digestion-, and ligation reactions were set up following the manufacturer's instructions. Chemical competent *E. coli* were prepared and transformed by heat shock as described by Sambrook and Russell (2001). *C. necator* cells were prepared and transformed by electroporation following a method reported by Ausubel et al. (2003) or by conjugation (Lenz et al., 1994).

### 2.3. Plasmid construction and gene integration

Plasmids were constructed by HiFi DNA assembly or conventional restriction enzyme-based cloning (Sambrook and Russell, 2001). The *P. putida mtlD/mlp* was amplified from *P. putida* KT2440 genomic DNA. EsM1PDH1cat (here termed *Esm1D*) and EsM1Pase2 (here termed *Esm1p*) were amplified from pESM1PDH1cat and pFEsM1Pase2, respectively (Bonin et al., 2015; Groisillier et al., 2014). The remaining *mtlD/mlp* genes were optimised for *E. coli* codon usage and synthesised (Thermo Fisher Scientific). Coding sequences can be found in Supplementary Table 2. The plasmids harbouring the mannitol production-detection systems contain: the genes encoding the mannitol- and arabinose-responsive transcriptional regulators MtlR and AraC, respectively, under control of their native promoters (Hoffmann and Altenbuchner, 2015; Schleif, 2000), the *rfp* reporter gene under control of the mannitol-inducible promoter  $P_{mtlE}$ , and the arabinose-controllable promoter  $P_{araBAD}$  (Supplementary Fig. 1). The version of  $P_{mtlE}$  used in this study harbours a mutation in the  $-35$  element resulting in a strong reduction in basal promoter activity whilst maintaining a high induction ratio (Hoffmann and Altenbuchner, 2015). To enhance *mtlD/mlp* gene expression through improved mRNA stability, the bacteriophage T7 gene 10 (T7g10) 5' untranslated region was introduced upstream of the *E. coli* consensus RBS sequence "ttaaagaaggagatatacat" (Bi et al., 2013).

Plasmids that were used for genomic integration of the mannitol biosynthesis pathway are derivatives of the suicide plasmid pLO3 (Lenz and Friedrich, 1998). They harbour *E. siliculosus mtlD/mlp* under control of the heterologous arabinose-inducible system or the native *phaC* promoter, flanked by homology arms of roughly 1000 bp each, being identical to the upstream and downstream regions of the integration site (Supplementary Fig. 2). Gene integrations were performed following the method described by Lenz and co-workers (Lenz et al., 1994).

All constructs were verified by PCR and Sanger sequencing (Source BioScience, Nottingham). A detailed assembly description for each plasmid is provided in the Supplementary Methods. Key features of all plasmids used and generated in this study are summarised in Supplementary Table 3. The nucleotide sequences of the plasmids pEH030, pEH031, pEH067, pEH140, pEH141, pEH142 and pEH145 have been deposited in the public version of the ACS registry (<https://acs-registry.jbei.org>) under the accession numbers ACS\_000867 to ACS\_000873, respectively.

### 2.4. Cultivation in small-volume cultures

For the initial screening of genes for mannitol biosynthesis in *C. necator* and the heterotrophic production of mannitol in small volumes, individual colonies of freshly transformed *C. necator* were used to inoculate 5 mL of MM containing chloramphenicol in 50-mL conical centrifuge tubes. Following incubation over night with orbital shaking at 200 rpm and 30 °C, cells were diluted to an OD<sub>600</sub> of 0.25 in fresh 10 mL of MM containing the respective antibiotic. After incubation for 1 h, each culture was split into two equal parts. L-arabinose was added to one culture to a final concentration of 0.02% (wt/vol), whereas the other one remained non-induced. As before, cells were incubated at 30 °C with orbital shaking at 200 rpm. Samples of 0.5 mL were taken 6, 24, and 48 h after supplementation with arabinose and used to quantify culture

OD<sub>600</sub>, RFP fluorescence and mannitol concentration using high performance liquid chromatography (HPLC).

### 2.5. Investigation of inducer range

For the mannitol biosensor-assisted investigation of inducer range, individual colonies of freshly transformed *C. necator* were used to inoculate 5 mL of LB medium containing chloramphenicol in 50-mL conical centrifuge tubes. Following incubation overnight with orbital shaking at 200 rpm and 30 °C, cells were diluted to an OD<sub>600</sub> of 0.05 in fresh 5 mL of LB containing the respective antibiotic. After incubation for 2 h, 142.5  $\mu$ L of culture were transferred to a well of a 96-well clear-bottom plate (Greiner Bio-One International). To each well, 7.5  $\mu$ L of arabinose stock solution were added to obtain the desired inducer concentration. Cells were incubated in an Infinite M1000 PRO micro plate reader (Tecan) with orbital shaking at 582 rpm and an amplitude of 1 mm and the temperature set at 30 °C. RFP fluorescence and culture OD<sub>600</sub> were measured from cells in late exponential growth phase after 8 h.

### 2.6. Cultivation in large-volume cultures and extraction of intracellular mannitol

For the heterotrophic production of mannitol in large volumes, pre-cultures were set up as for the mannitol biosensor-assisted investigation of inducer range. The overnight culture was diluted 1:50 into fresh LB medium containing chloramphenicol. Cultures were grown in 50-mL volumes in 250-mL baffled shake flasks with orbital shaking at 200 rpm and 30 °C. At an OD<sub>600</sub> of 0.2-0.4, 100  $\mu$ L of arabinose stock solution were added to obtain the desired inducer concentration. Samples were taken 12 h after supplementation with arabinose and used to quantify culture OD<sub>600</sub> and mannitol concentration using HPLC. To determine the intracellular mannitol concentration, the culture volume corresponding to an OD<sub>600</sub> of 50 was centrifuged for 10 min at 16,000g. The cell pellet was washed in 1 mL of phosphate buffered saline, transferred to a microcentrifuge tube and centrifuged as before. Subsequently, the supernatant was completely removed, the pellet was weighed using fine balance and frozen overnight at  $-80$  °C. Extraction and calculation of intracellular mannitol concentration was performed as described previously (Hanko et al., 2018).

### 2.7. Cultivation in bioreactors

Autotrophic batch fermentation of *C. necator* was performed as reported previously by Gascoyne and co-workers (Gascoyne et al., 2021) with slight modifications. Briefly, to prepare the fermenter culture, individual colonies of freshly streaked *C. necator* were used to inoculate 5 mL of LB medium containing gentamycin in 50-mL conical centrifuge tubes. To set up the fermenter inoculum, 1 mL of overnight culture was transferred into 120 mL of SOB medium containing gentamycin. Following incubation overnight with orbital shaking at 200 rpm and 30 °C, cells were harvested by centrifugation at 10,000g for 10 min, washed once in 40 mL of modified DSMZ 81 medium (Bommareddy et al., 2020), centrifuged as before and resuspended in 50 mL of modified DSMZ 81 medium. Subsequently, the resuspended cells were used to inoculate the bioreactor with a total working volume of 750 mL. Expression of *E. siliculosus mtlD/mlp* in strains NM0010 and NM0011 was induced by addition of arabinose to a final concentration of 5 mM at dry cell weights (DCWs) greater than 1 g/L. To limit nitrogen availability the base was switched from 1 M NH<sub>4</sub>OH to 1 M KOH at DCWs of 2 g/L.

### 2.8. Fluorescence measurements

To quantify RFP fluorescence, unless directly grown in a microtitre plate, 100  $\mu$ L of cells were transferred to a 96-well clear bottom plate

and fluorescence and OD<sub>600</sub> were quantified using an Infinite M1000 PRO micro plate reader. Fluorescence excitation and emission wavelengths were set to 585 nm and 620 nm, respectively. For fluorescence measurements in minimal medium the gain factor was set manually to 100%, whereas for rich medium it was set to 80% unless indicated otherwise. Culture optical density was measured at 600 nm to normalise RFP fluorescence by optical density. To account for media autofluorescence and –optical density, fluorescence and OD<sub>600</sub> values were corrected by subtracting the fluorescence and OD<sub>600</sub> of the cell-free culture medium prior to normalisation.

## 2.9. Analytical methods

Samples for HPLC analysis were prepared by combining cell-free supernatants with an equal volume of mobile phase spiked with 50 mM valerate as internal standard. The mobile phase was composed of 5 mM H<sub>2</sub>SO<sub>4</sub>. Subsequently, the mixture was passed through a cellulose acetate syringe filter with a pore size of 0.22 μm. Samples were analysed using a Thermo Scientific UltiMate 3000 HPLC system equipped with a Phenomenex Rezex ROA-organic acid H+ (8%) 150 mm × 7.8 mm × 8 μm column, a diode array detector DAD-3000 with the wavelengths set at 210 and 280 nm and a refractive index detector RefractoMax 521 (Thermo Fisher Scientific). The flow rate of the mobile phase was set to an isocratic 0.5 mL/min with a column temperature of 35 °C. Samples were run for 30 min and the injection volume was 20 μL. Data analysis was performed using Chromeleon 7 (Thermo Fisher Scientific). Mannitol concentrations were quantified using calibration curves generated from running standards of known concentrations, which were prepared the same as the samples.

DCW was quantified by pelleting 1 mL of cell culture in a pre-dried and pre-weighed 1.5 mL Eppendorf tube. The supernatant was removed, and the cell pellet was dried for 48 h at 100 °C and weighed using a fine balance. DCW was calculated as grams per litre.

## 2.10. Mathematical modelling

To obtain biosensor dose-response parameters, normalised fluorescence values were plotted as a function of mannitol concentration using software GraphPad Prism 7. A non-linear least-squares fit was performed using Hill function:

$$\text{RFP}(I) = b_{\max} \times \frac{I^h}{K_m^h + I^h} + b_{\min}$$

Parameters correspond to the maximum level of biosensor output ( $b_{\max}$ ), the concentration of mannitol ( $I$ ), the Hill coefficient ( $h$ ), the mannitol concentration mediating half-maximal biosensor output ( $K_m$ ), and the basal level of fluorescence output ( $b_{\min}$ ).

## 3. Results

### 3.1. Screening of genes for mannitol biosynthesis in *C. necator*

The biosynthesis of mannitol from fructose 6-phosphate (F-6-P) involves two catalytic steps (Fig. 1A). First, F-6-P is reduced to mannitol 1-phosphate (Mtl-1-P) by the action of a Mtl-1-P dehydrogenase (MtlD, also commonly referred to as M1PDH). Subsequently, Mtl-1-P is dephosphorylated by Mtl-1-P phosphatase (M1P, also referred to as M1Pase), forming mannitol. This mannitol biosynthetic pathway from F-6-P, involving two independent enzymes, has been characterised in homofermentative lactic acid bacteria (Neves et al., 2000), algae (Iwamoto et al., 2003), and Apicomplexa (Schmatz et al., 1989). Recently, an MtlD/M1P fusion protein from *Acinetobacter baylyi* ADP1 has been shown to catalyse both enzymatic reactions, F-6-P reduction and Mtl-1-P dephosphorylation (Sand et al., 2015). Bioinformatic analysis of the bifunctional enzyme revealed a haloacid dehalogenase-like phosphatase domain at the N-terminus being unique to previously reported MtlDs (Sand et al., 2015). As enzymes with the same catalytic function from different organisms often exhibit distinct catalytic efficiencies, we sought to test a number of combinations of monofunctional MtlD/M1Ps, as well as bifunctional fusion MtlD/M1Ps for their ability to produce mannitol in *C. necator* (Supplementary Table 4).

The first pair of monofunctional enzymes that was tested for mannitol production originates from the model brown alga *Ectocarpus siliculosus*. Previously, its N-terminal domain of 142 amino acids was shown to be non-essential for *E. siliculosus* MtlD enzymatic function (Bonin et al., 2015; Rousvoal et al., 2011). Therefore, a truncated version of *E. siliculosus* mtlD, reduced to solely encode the catalytic domain of the enzyme (Bonin et al., 2015; Rousvoal et al., 2011), was co-expressed with *E. siliculosus* m1p2 (Groisillier et al., 2014). The second pair of monofunctional enzymes was sourced from the protozoan

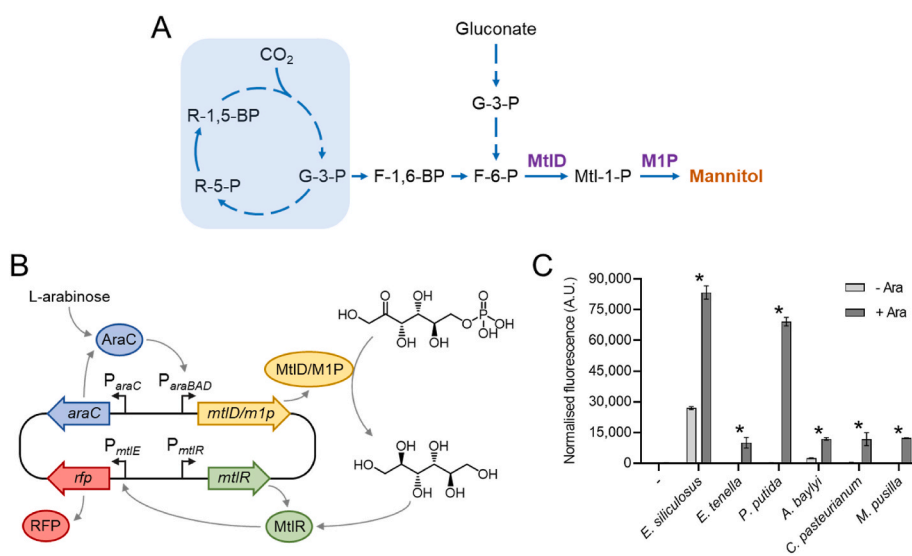


**Fig. 1.** Screening of genes for mannitol biosynthesis in *C. necator*. **A** Pathway for the production of mannitol in *C. necator* under autotrophic growth conditions via the Calvin-Benson-Bassham cycle (highlighted in blue) and under heterotrophic growth conditions via gluconate as carbon source. R-1,5-BP, Ribulose 1,5-bisphosphate; G-3-P, Glyceraldehyde 3-phosphate; R-5-P, Ribulose 5-phosphate; F-1,6-BP, Fructose 1,6-bisphosphate; F-6-P, Fructose 6-phosphate; Mtl-1-P, Mannitol 1-phosphate; MtlD, mannitol 1-phosphate dehydrogenase; M1P, mannitol 1-phosphate phosphatase. **B** Example of a vector harbouring the mannitol biosensor and the mannitol biosynthetic gene/s under control of the L-arabinose-inducible system. Addition of arabinose results in production of MtlD/M1P, catalysing the conversion of F-6-P into mannitol. MtlR consequently mediates expression of the red fluorescent protein (RFP) reporter gene in response to mannitol. **C** Normalised RFP fluorescence values of *C. necator* carrying the mannitol production-sensor vector with *mtlD/m1p* genes from a range of different organisms (see Supplementary Table 4). Cells were grown in minimal medium. RFP fluorescence output was quantified in the absence of arabinose (-Ara) and 24 h after supplementation with arabinose (+Ara).

to a final concentration of 0.02% (wt/vol). -, negative control vector pEH031 lacking *mtlD/m1p*. Error bars represent standard deviations of three biological replicates. Asterisks indicate statistically significant induction values for  $p < 0.005$  (unpaired *t*-test).

chicken parasite *Eimeria tenella*. *E. tenella* M1P was previously employed in combination with the *Escherichia coli* MtlD for the production of mannitol in *Synechococcus* sp. PCC 7002 (Jacobsen and Frigaard, 2014) and *E. coli* itself (Reshamwala et al., 2014). Here, mannitol biosynthesis was investigated upon expression of *E. tenella* *m1p* in combination with *E. tenella* *mtlD*. Due to a sequence of poly-serines, most likely resulting in poor translational efficiency, and protein sequence homology to the non-catalytic N-terminal domain of *E. siliculosus* MtlD (Rousvoal et al., 2011), the *E. tenella* MtlD was truncated by 43 residues ranging from A438 to L479 and by 168 residues at the N-terminus, respectively. Deletion of amino acids was performed in such way that the *E. tenella* MtlD protein sequence aligns with *E. siliculosus* MtlD and other species homologues without gaps in the sequence region where amino acids were removed. The bifunctional enzymes that were investigated for mannitol biosynthesis were obtained from the following organisms: the soil bacteria *Pseudomonas putida*, *Acinetobacter baylyi*, and *Clostridium pasteurianum*, as well as the green alga *Micromonas pusilla*. The bifunctional enzyme of the latter has been demonstrated to facilitate mannitol production in both *E. coli* and *Synechococcus* sp. PCC 7002 (Madsen et al., 2018). As for *E. tenella* MtlD, the *M. pusilla* MtlD/M1P was truncated by 73 residues at the N-terminus to align with the catalytic domain of *E. siliculosus* MtlD.

To facilitate mono- and bifunctional MtlD/M1P screening under different expression conditions, corresponding genes were cloned into vector pEH031 (Supplementary Table 3, Supplementary Fig. 1) that contains a mannitol biosensor, enabling the *in vivo* monitoring of mannitol formation by red fluorescent protein (RFP) fluorescence output. Implementation of a mannitol biosensor offers the advantage that individual parameters affecting product biosynthesis, including enzyme turnover number or gene expression level, can be rapidly evaluated. Expression of the mannitol biosynthesis pathway is controlled by the L-arabinose-inducible system (Fig. 1B). Supplementation of the growth medium with arabinose initiates expression of *mtlD/m1p*, the translational product/s of which catalyse/s the conversion of F-6-P to mannitol. Subsequently, the mannitol-responsive transcriptional regulator MtlR activates expression of the *rfp* reporter gene from its corresponding promoter  $P_{mtIE}$  (Hoffmann and Altenbuchner, 2015). To gain an initial overview of which enzymes catalyse the biosynthesis of mannitol, *C. necator* cells carrying the mannitol production-sensor vectors were grown in the absence and presence of arabinose and RFP fluorescence was monitored. All constructs harbouring *mtlD/m1p* genes showed a statistically significant induction of reporter gene expression 24 h after supplementation with arabinose (Fig. 1C). The highest level of fluorescence was achieved by *E. siliculosus* MtlD/M1P, followed by *P. putida* MtlD/M1P, exceeding fluorescence levels of the other enzyme candidates tested by more than 5-fold. Except for *E. siliculosus* and *A. baylyi* MtlD/M1P, resulting in considerable levels of background fluorescence output, reporter gene expression in the absence of arabinose was comparable to the negative control plasmid lacking *mtlD/m1p*. The functionality of the mannitol-sensor module was confirmed by extracellular addition of D-mannitol to cells carrying the negative control plasmid pEH031. Whereas supplementation of the growth medium with 0.2% (wt/vol) mannitol led to a 97-fold increase in RFP fluorescence (Supplementary Fig. 3), addition of arabinose to cells carrying pEH031 did not induce reporter gene expression (Fig. 1C, Supplementary Fig. 3). This suggests that an increase in fluorescence output in response to arabinose is caused by biosynthesis of mannitol rather than cross-induction of the mannitol sensor by arabinose. Moreover, to determine its detection range, cultures of *C. necator* solely carrying the mannitol biosensor, pEH003, were subjected to a range of mannitol concentrations and RFP fluorescence and optical density at 600 nm ( $OD_{600}$ ) were quantified for cells in exponential growth phase. The dose-response was obtained by plotting the normalised fluorescence values as a function of mannitol concentration and data points were fit using a Hill function (see Methods). When extracellularly added to cells harbouring the biosensor, the mannitol concentration that mediated

half-maximal biosensor output,  $K_m$ , was 3.7 mM (Supplementary Fig. 4). The concentrations of mannitol falling within 10% and 90% of the maximum level of biosensor output,  $b_{max}$ , ranged from 1.2 mM to 9.7 mM. It should be noted, however, that the amount of mannitol with which the medium was supplemented may differ from the intracellular mannitol concentration mediating the biosensor output.

### 3.2. Heterotrophic production of mannitol in small volumes

To confirm the observations of the initial enzyme screen, mannitol titres were quantified in cultures of *C. necator* carrying the various mannitol production-sensor vectors. Cells were grown in 5-mL cultures of minimal medium with 0.4% (wt/vol) gluconate as sole carbon source and expression of *mtlD/m1p* was induced by addition of L-arabinose to a final concentration of 0.02% (wt/vol). Mannitol could be detected in the culture supernatants of all strains tested. However, final mannitol titres varied greatly from 7 mg/L (*M. pusilla* MtlD/M1P) to 429 mg/L (*E. siliculosus* MtlD/M1P) with the latter strain (Fig. 2) resulting in a molar yield of 0.13 [(mol mannitol)/(mol gluconate)] at 24 h. Whereas mannitol titres remained below the detection limit until the 24 h after addition of arabinose for cells expressing *mtlD/m1p* from *E. tenella*, *C. pasteurianum*, and *M. pusilla*, mannitol could be detected after 6 h in the cultures of the three best performing strains producing *E. siliculosus*, *P. putida*, and *A. baylyi* MtlD/M1P. In addition, mannitol was produced by these three strains even in the absence of arabinose with cells expressing *E. siliculosus* *mtlD/m1p* forming 21.6 mg/L mannitol at the 24 h time point (Supplementary Table 5).

### 3.3. Mannitol biosensor-assisted investigation of inducer range

Using inducible promoters for controlling expression of biosynthetic pathways offers the advantage that the level of gene expression can be fine-tuned as it is a function of inducer concentration. Balancing gene expression is often crucial to avoid negative effects from accumulated intermediate products and to ensure optimal metabolic flux (Lee et al., 2013). Here, expression of the heterologous *mtlD/m1p* gene/s is mediated by the arabinose-inducible system, which was previously shown to be highly operable in the range between 0.016 and 2.5 mM in *C. necator* (Alagesan et al., 2018a). To determine the effect of varying inducer concentrations on both mannitol biosensor output and cell viability, strains of *C. necator* carrying the various mannitol production-detection systems were subjected to a wide range of arabinose concentrations and RFP fluorescence and  $OD_{600}$  were quantified for cells in late exponential growth phase. In contrast to the initial screen of enzyme candidates (Fig. 1C), which was performed in minimal medium with gluconate as carbon source, the investigation of arabinose-inducer range was conducted in rich medium. It should be noted that the inducer concentration, at which the induction rate of the arabinose-inducible system is 50%, is similar for *C. necator* cells grown either in minimal or rich medium as reported previously (Alagesan et al., 2018a; Johnson et al., 2018). Moreover, considering that in response to a higher availability of nutrients cells in rich medium generally grow faster and the expression of housekeeping genes, including translation apparatus genes, is elevated (Tao et al., 1999), the use of rich medium enabled to establish whether the biosynthesis of mannitol can be improved by enriching growth medium and validate the best mannitol production systems.

For cells grown in complex medium, two different biosensor output patterns could be observed (Fig. 3). In the absence of arabinose, cells expressing *mtlD/m1p* from *E. tenella*, *P. putida*, and *M. pusilla* exhibited fluorescence outputs at the level of the negative control vector (Supplementary Table 6). An increase in arabinose concentrations up to 10 mM generally led to an increase in normalised fluorescence, with the exception of cells producing *E. tenella* MtlD/M1P demonstrating maximum normalised fluorescence levels at 1.25 mM arabinose. In contrast, the biosensor output resulting from expression of *E. siliculosus*, *A. baylyi*, and *C. pasteurianum* *mtlD/m1p* was constant within the range

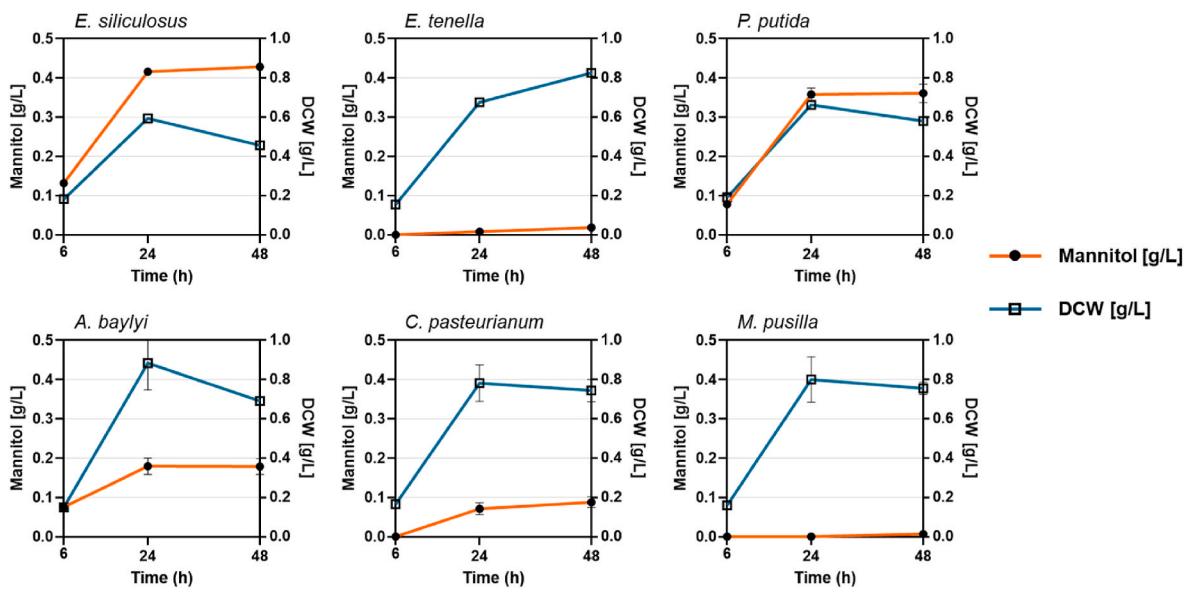


**Fig. 2.** Mannitol biosynthesis of *C. necator* carrying plasmids pEH067, pEH145, pEH030, pEH140, pEH142 and pEH141 with *mtID/mIP* from *E. siliculosus*, *E. tenella*, *P. putida*, *A. baylyi*, *C. pasteurianum* and *M. pusilla*, respectively, under control of the arabinose-inducible system. Cells were grown in minimal medium supplemented with 0.4% (wt/vol) sodium gluconate as sole carbon source. Samples were taken 6, 24, and 48 h after addition of arabinose to a final concentration of 0.02% (wt/vol), and mannitol (circle) and dry cell weight (DCW; square) were quantified. Results are the average of three biological replicates with error bars representing the standard deviation from the mean.

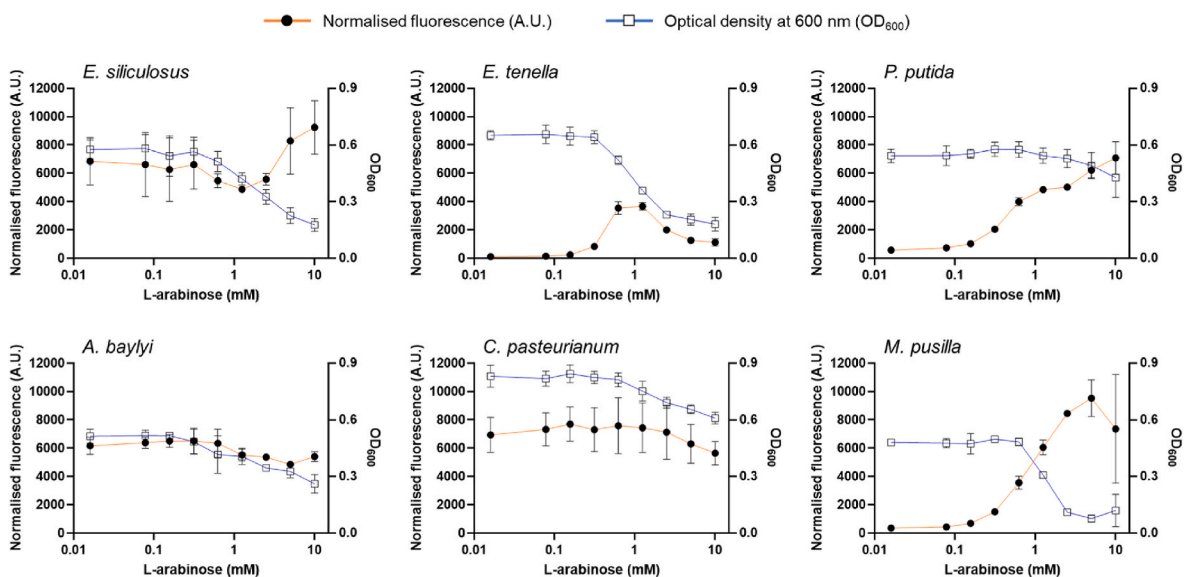


**Fig. 3.** Fluorescence output and growth of *C. necator* cells, carrying plasmids pEH067, pEH145, pEH030, pEH140, pEH142 and pEH141 with *mtID/mIP* from *E. siliculosus*, *E. tenella*, *P. putida*, *A. baylyi*, *C. pasteurianum* and *M. pusilla*, respectively, at different arabinose concentrations. Strains were grown in LB medium. Fluorescence (circle) and OD<sub>600</sub> (square) were quantified from cells in late exponential growth phase. The growth medium was supplemented with arabinose at the following final concentrations: 0.019, 0.078, 0.156, 0.313, 0.625, 1.25, 2.5, 5, and 10 mM. Fluorescence and OD<sub>600</sub> values of the non-induced cultures can be found in [Supplementary Table 6](#). Results are the average of three biological replicates with error bars representing the standard deviation from the mean.

of error for all arabinose concentrations tested. Maximum fluorescence levels normalised by culture OD<sub>600</sub> for the individual *MtID/M1P*s (and their corresponding arabinose concentrations) were as follows: *E. tenella*, 3678 ± 277 (1.25 mM); *E. siliculosus*, 9231 ± 1890 (10 mM); *P. putida*, 7087 ± 1144 (10 mM); *A. baylyi*, 6509 ± 457 (0.156 mM); *C. pasteurianum*, 7692 ± 1205 (0.156 mM); *M. pusilla*, 9526 ± 1293 (5 mM).

A similar effect on cell growth could be observed for all mannitol biosynthetic genes with an increase in arabinose concentration resulting in reduced cell density (Fig. 3). Supplementation of wild type *C. necator* cells with 10 mM arabinose did not affect cell growth (data not shown).

Expressing the different candidate genes using a range of inducer concentrations, however, reduced cell viability from 19% (*P. putida mtID/m1p*) to up to 84% (*M. pusillaa mtID/m1p*, at 5 mM arabinose).

#### 3.4. Heterotrophic production of mannitol in large volumes

Based on the results of the initial enzyme screen (Fig. 2), the three best performing strains were selected to be analysed for mannitol biosynthesis in heterotrophic shake flask cultures. Informed by the biosensor-assisted evaluation of inducer range, mannitol production was quantified in response to three different inducer concentrations. They

were chosen for each strain individually to reflect what was presumed to be the optimum level of induction, exhibiting a high fluorescence output whilst maintaining a high cell viability (e.g. 0.625 mM, 0.625 mM, and 0.156 mM arabinose for *P. putida*, *E. siliculosus* and *A. baylyi* *mtlD/m1p*, respectively), as well as one inducer concentration below and one above this level. *C. necator* carrying the mannitol production-detection vectors was grown in 50 mL of LB. Arabinose was added to exponentially growing cells (OD<sub>600</sub> of 0.2–0.4) and samples were taken 12 h after inducer addition. To investigate the cells' ability to export the final product, mannitol was quantified in both culture supernatant and cell pellet.

In all three strains tested, supplementation of the growth medium with the highest arabinose concentration resulted in the highest mannitol titre (Fig. 4A). With the exception of *P. putida* *mtlD/m1p* expressed at 0.156 mM arabinose, showing a 52/48 split between the extra- and intracellular fraction, the majority of mannitol of at least 80% was found in the culture supernatants (Fig. 4B). Mannitol titres at the highest arabinose concentrations tested were 54 mg/L, 245 mg/L, and 277 mg/L in culture supernatants of cells expressing *mtlD/m1p* from *P. putida*, *E. siliculosus*, and *A. baylyi*, respectively. Similar to what has been observed for cells grown in small volumes of minimal medium (Supplementary Table 5), mannitol could be detected in cultures of cells carrying *E. siliculosus* and *A. baylyi* *mtlD/m1p* in the absence of arabinose. These results are consistent with the outcome of the biosensor-assisted investigation of inducer range where *C. necator* expressing *E. siliculosus* and *A. baylyi* *mtlD/m1p* demonstrated a considerable fluorescence reporter output even under non-inducing conditions (Supplementary Table 6). As the leakiness from the arabinose-inducible promoter may be considered the same between all gene candidates tested, biosynthesis of mannitol under non-inducing conditions suggests a higher translational or catalytic efficiency of *E. siliculosus* and *A. baylyi* *MtlD/M1P*. Because of its overall performance in both minimal and complex media, *mtlD/m1p* from *E. siliculosus* was selected to be analysed for autotrophic production of mannitol in batch fermentations.

### 3.5. Autotrophic production of mannitol

To investigate whether F-6-P, generated via the Calvin-Benson-Bassham (CBB) cycle during autotrophic growth, can be redirected toward mannitol biosynthesis, *E. siliculosus* *mtlD/m1p* was integrated into the chromosome of *C. necator*. In total, three strains were generated (Table 1, Supplementary Fig. 2). In strain NM0010, the *phaCAB* operon, encoding the proteins for the biosynthesis of PHB, was replaced by

*E. siliculosus* *mtlD/m1p* under control of the heterologous arabinose-inducible system. To investigate the impact of constitutive expression of the mannitol biosynthetic genes on product formation, *E. siliculosus* *mtlD/m1p* were cloned downstream of the native *phaC* promoter, thereby replacing the *phaCAB* operon, yielding strain NM0013. A second integration site was selected to determine if the presence of *C. necator*'s natural carbon sink pathway to PHB had any adverse effects on mannitol production. Consequently, the *tcuAB* operon, encoding proteins putatively involved in tricarballoylate catabolism, was replaced by *E. siliculosus* *mtlD/m1p* under control of the arabinose-inducible system, yielding strain NM0011. In contrast to NM0010 and NM0013, in strain NM0011 the *phaCAB* operon is intact.

Bioreactors were inoculated at an optical density of 1 with cells resuspended in mineral medium for chemolithotrophic growth. Both H<sub>2</sub> and CO<sub>2</sub> were fed at a rate of 35.1 L/h and 1.35 L/h, respectively. O<sub>2</sub> was fed through air at a variable rate controlled by the off-gas O<sub>2</sub> concentration, which was set at 4% (v/v). To induce expression of *E. siliculosus* *mtlD/m1p* in strains NM0010 and NM0011, arabinose was added to cells in exponential growth phase to a final concentration of 5 mM. After 167 h of autotrophic fermentation, the final concentrations of dry cell weight (DCW) were 5.5 g/L, 14.2 g/L, and 4.9 g/L for strains NM0010, NM0011, and NM0013, respectively (Fig. 5A). Strains NM0010 and NM0013 reached a maximum concentration of DCW after 71 h, whereas in the PHB-producing strain, NM0011, biomass continued to increase until the 143 h time point. Mannitol was produced in all three strains as indicated by the absolute mannitol titres and specific productivity on a biomass basis (Fig. 5B and C). Strain NM0013 ( $\Delta$ *phaCAB* *P*<sub>*phaC*</sub>-*mtlD/m1p*) started producing mannitol immediately after inoculation and exhibited a constant level of productivity ranging from 0.036 [(mmol mannitol)/(gDCW·h)] to 0.054 [(mmol mannitol)/(gDCW·h)] between 17 h and 71 h. The strains NM0010 ( $\Delta$ *phaCAB* *P*<sub>*araBAD*</sub>-*mtlD/m1p*) and NM0011 ( $\Delta$ *tcuAB* *P*<sub>*araBAD*</sub>-*mtlD/m1p*) reached a maximum specific productivity of 0.069 [(mmol mannitol)/(gDCW·h)] and 0.06 [(mmol mannitol)/(gDCW·h)], respectively, roughly 30 h after arabinose had been added, followed by a slow decrease in productivity until the end of cultivation. Final mannitol titres were 3.9 g/L, 3.3 g/L, and 2.6 g/L for strains NM0010, NM0011, and NM0013, respectively. This represented final yields of 0.71 [(g mannitol)/(g DCW)], 0.23 [(g mannitol)/(g DCW)], and 0.53 [(g mannitol)/(g DCW)], respectively, after 167 h of gas fermentation. From 53.5 h to 71 h, strains NM0010, NM0011, and NM0013 achieved molar carbon yields of 0.48 [(C-mol mannitol)/(C-mol CO<sub>2</sub>)], 0.16 [(C-mol mannitol)/(C-mol CO<sub>2</sub>)] and 0.26 [(C-mol mannitol)/(C-mol CO<sub>2</sub>)] (Fig. 5D), respectively, and increased further

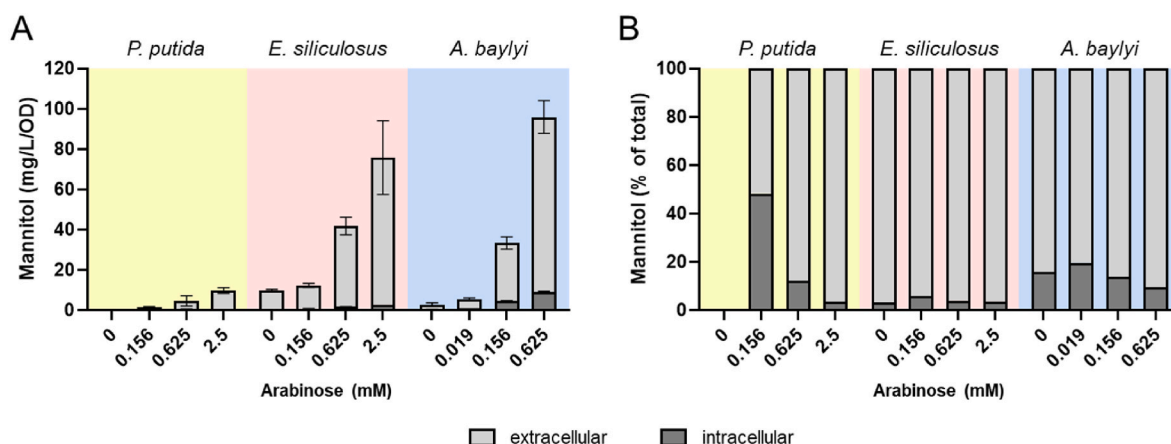
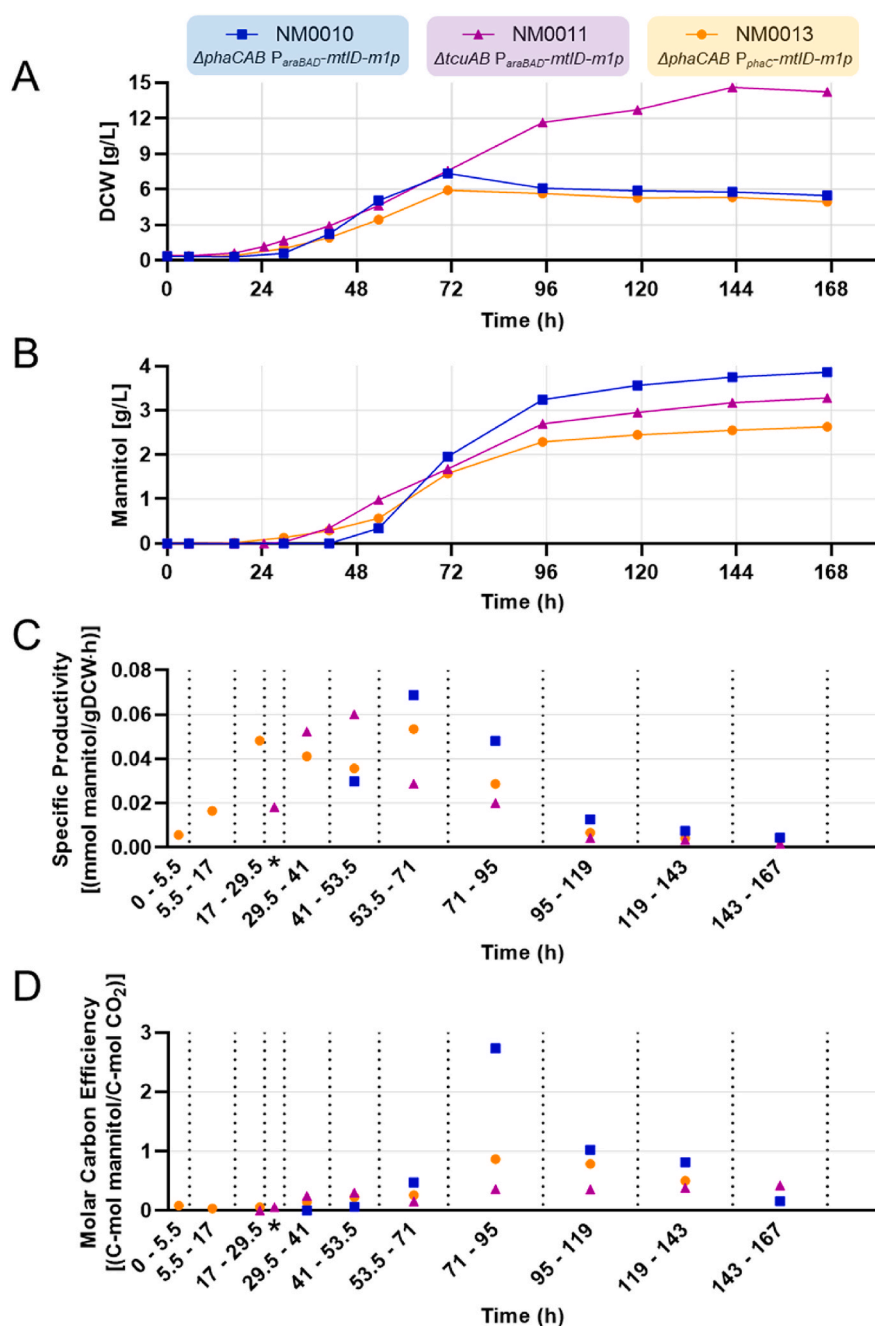


Fig. 4. Mannitol biosynthesis in heterotrophic shake flask cultures of *C. necator* carrying plasmids pEH030, pEH067 and pEH140 with *mtlD/m1p* from *P. putida*, *E. siliculosus*, and *A. baylyi*, respectively, under control of the arabinose-inducible system. **A** Specific production, **B** Mannitol split between culture supernatant and cell pellet (in % of total). Cells were grown in 50 mL of LB supplemented with arabinose at the concentrations indicated. Samples were taken 12 h after addition of arabinose and mannitol was quantified. No mannitol was detected in cells carrying *P. putida* *mtlD/m1p* in the absence of arabinose. Results are the average of three biological replicates with error bars representing the standard deviation from the mean.



**Fig. 5.** Biosynthesis of mannitol by controlled gas fermentation. Production data from batch fermentations of NM0010 ( $\Delta\text{phaCAB } P_{\text{araBAD}}\text{-mtlD-}m1p$ ; blue square), NM0011 ( $\Delta\text{tctuAB } P_{\text{araBAD}}\text{-mtlD-}m1p$ ; purple triangle), and NM0013 ( $\Delta\text{phaCAB } P_{\text{phaC}}\text{-mtlD-}m1p$ ; orange circle). **A** Dry cell weight, **B** mannitol titre. To induce gene expression, arabinose was added 41 h and 24.5 h after fermenter inoculation with strains NM0010 and NM0011, respectively. **C** Specific productivity and **D** molar carbon efficiency are given for the time frames from 0 to 5.5, 5.5 to 17, 17 to 29.5, 29.5 to 41, 41 to 53.5, 53.5 to 71, 71 to 95, 95 to 119, 119 to 143, and 143 to 167 h. Asterisk shows the time frame from 24.5 to 29.5 h in case of NM0011.

throughout the cultivation as mannitol titres continued to rise. In the time frame 71 h–95 h, the specific  $\text{CO}_2$  uptake rate dropped significantly during fermentation of strain NM0010 (Supplementary Fig. 5). This was coupled with a decrease in biomass and an increase in mannitol titre (Fig. 5A and B), consequently resulting in a molar carbon yield of 2.74 [(C-mol mannitol)/(C-mol  $\text{CO}_2$ )]. It should be noted that no extracellular by-products were observed for any of the strains throughout their cultivation.

#### 4. Discussion

The utilisation of  $\text{CO}_2$  as a feedstock for the biosynthesis of chemicals and fuels is critically important seeking to reduce greenhouse gas emissions and re-cycle combustible waste. However, considering the enormous amount of basic and applied research that has been carried out on the bioproduction and biotechnology of chemical compounds,

there is a limited number of examples where  $\text{CO}_2$  is utilised as a carbon source. Nonetheless, alongside cyanobacteria, chemolithoautotrophic bacterium *C. necator* H16 has attracted significant attention for its ability to accumulate large quantities of PHB under excess carbon and utilise  $\text{CO}_2$  as sole carbon source.

Mannitol is industrially either extracted from seaweed or produced chemically by hydrogenation of fructose. It is ranked as one of the top twenty bio-based chemical opportunities in the UK (E4tech (UK) Ltd for LBNet, 2017). In this study, *C. necator* H16 transformed with a set of plasmids was utilised as a microbial chassis and whole cell biosensor to screen several mannitol biosynthesis genes. Of the investigated genes *E. siliculosus*, *A. baylyi*, and *P. putida mtlD/m1p* variants were identified as most prominent for mannitol production in *C. necator* H16. Subsequently, we engineered *C. necator* H16 by integrating *mtlD* and *m1p2* from *E. siliculosus* for autotrophic production of mannitol from  $\text{CO}_2$ . Three engineered strains achieved final titres from 2.6 to 3.9 g/L



mannitol. The highest producing strain showed an average productivity of 94.2 mg/L/h and yield of 0.48 [(C-mol mannitol)/(C-mol CO<sub>2</sub>)] from 53.5 h to the 71 h time point of fermentation. These titres, productivity and yield are substantially higher than those reported for mannitol production from CO<sub>2</sub> in recombinant cyanobacteria (Table 2) and they are in the same range with the high productivities of *C. necator* H16 reported for chemicals such as acetoin (Windhorst and Gescher, 2019), 1,3-butanediol (Gascoyne et al., 2021), 2,3-butanediol (Bommareddy et al., 2020) and isopropanol (Marc et al., 2017). The mannitol yield was improved in the  $\Delta$ phaCAB strains (Fig. 5D). Inactivation of PHB biosynthesis resulted in a relatively lower biomass production whilst increasing CO<sub>2</sub> conversion into mannitol by 2–3-fold. From the 71 h time point the molar carbon yield of strains NM0010 and NM0013 increased further and significantly above 0.48 [(C-mol mannitol)/(C-mol CO<sub>2</sub>)] throughout the fermentation as mannitol titres continued to rise. Similarly, as reported for acetoin (Windhorst and Gescher, 2019), the abolishment of PHB synthesis enabled to engineer a strain that was able to produce mannitol with a maximum molar carbon yield close to 1.0 [(C-mol mannitol)/(C-mol CO<sub>2</sub>)]. It should be noted that a transient increase of estimated molar carbon efficiency above theoretical maximum was observed between 71 h and 95 h for strain NM0010 most likely due to the decrease of cell optical density and potential utilisation of the intracellular carbon accumulated in the early phase of fermentation.

The use of the CBB cycle for CO<sub>2</sub> fixation allows theoretically up to 100% carbon efficiency during mannitol biosynthesis as the pool of glyceraldehyde 3-phosphate (G-3-P), available for fructose 6-phosphate formation, is continuously replenished. This is supported by reverse activity (gluconeogenesis) of the upper part of the Embden-Mayerhof-Parnas (EMP) pathway as a consequence of the absence of phosphofructokinase in *C. necator* H16 (Alagesan et al., 2018b). Consistent with this, other products derived from pyruvate, including acetoin (Windhorst and Gescher, 2019), 1,3-butanediol (Gascoyne et al., 2021), or 2,3-butanediol (Bommareddy et al., 2020), also showed relatively high titres in engineered *C. necator* H16. Nonetheless, a relatively low turnover number of ribulose-1,5-bisphosphate carboxylase-oxygenase (RuBisCO) limits the rate of productivity. An improved titre of autotrophic mannitol production was achieved by the introduction of the most active combination of mannitol 1-phosphate dehydrogenases and mannitol 1-phosphate phosphatases, which were identified on the basis of a rigorous comparison of enzymes from bacteria and protista. They exhibited significant differences in either catalytic activities, expression levels or both, resulting in a large variation of mannitol biosynthesis in *C. necator* H16 (Figs. 1C and 2).

To establish whether the achieved maximum productivity of 94.2 mg/L/h is practical, we calculated that 710 g of mannitol can be produced per 1 kg of bacterial DCW in a 0.2 m<sup>3</sup> bioreactor within one week. Compared with mannitol production from seaweed, with only 300 g extracted from 1 kg of seaweed DCW, cultivation of which would require 30 m<sup>2</sup> of near-shore sea area based on previous estimations (Wei et al., 2013; Milledge et al., 2019), the mannitol productivity of engineered *C. necator* H16 is very promising. Although the hydrogenotrophic energy generation process used by this bacterium may not be as efficient as in acetogens (Nybo et al., 2015), it can be approximately 5 times higher

than the phototrophic energy generation process. It has been estimated that the *C. necator* H16-based electrosynthetic conversion gives a solar-to-product efficiency of approximately 7.6%, whereas solar-to-product conversion efficiencies of photosynthetic species is approximately 1.5% (Claessens et al., 2016).

Here we also demonstrated that the application of a fluorescence-based biosensor can provide valuable information on the biosynthesis pathway activity through the monitoring of product formation (Fig. 3). It enables to probe the change of pathway activity triggered by the differentiation of gene expression levels. The biosensor approach can be utilised for other biosynthetic pathways with more complex metabolic networks and involving rationally designed perturbation experiments. Compared with other approaches, the fluorescence-based biosensor technique enables relatively easy quantification of substrate, metabolic intermediate or product change intracellularly and extracellularly under *in vivo* conditions.

Moreover, this study shows that produced mannitol is excessively excreted into the culture medium (Supplementary Table 7). When 2.73 mg/L/OD or more mannitol is synthesised, at least 80% of mannitol is excreted. This further increases to over 95% at higher concentrations of mannitol. *C. necator* H16 is well known to release low-molecular-weight metabolites such as pyruvate (Raberg et al., 2014) or butanediols (Gascoyne et al., 2021), but not disaccharide trehalose (Löwe et al., 2021). As recently shown, trehalose was not released from salt-stressed *C. necator* H16 and the secretion was only achieved when the sugar efflux transporter *setA* from *E. coli* was expressed (Löwe et al., 2021). However, mannitol is a smaller molecule than the trehalose and appears not to require a specific transporter for extracellular release. Nonetheless, the mechanism of metabolite excretion has not been well characterised despite its great importance to industrial processes development and research has mainly been limited to amino and non-amino organic acid secretion (Pinu et al., 2018). Similarly, a mannitol-specific transporter has not been identified in *C. necator* H16. However, it is likely that low-molecular-weight metabolites, including mannitol, can be released due to hypo-osmotic stress when cells are subjected to a high intracellular concentration. This process might also involve activation of large- and small-conductance mechano-sensitive channels (Kung et al., 2010), genes of which are present in *C. necator* H16, i.e. *mscL* (H16\_A3399) and *mscS1* (H16\_A3040), *mscS2* (H16\_B0712), *mscS3* (H16\_B1233), *mscS4* (H16\_B1855) and *mscS5* (H16\_B2568).

Finally, due to the highly efficient G-3-P flow of the CBB cycle demonstrated in this study using the example of mannitol production via fructose 6-phosphate intermediate (Fig. 1A), the *C. necator* H16 strains developed here can serve as a platform for autotrophic production of hexoses and their derivatives. This work proofs an essential step toward constructing an autotrophic cell factory for the production of sugar derivatives from CO<sub>2</sub>.

## 5. Conclusions

D-Mannitol is a natural sugar alcohol used as a food additive, surfactant and in pharmaceutical applications. Increasing demand for bio-based products attracts this compound as one of the top chemical opportunities (E4tech (UK) Ltd for LBN, 2017). Here we engineered

**Table 2**

Production of mannitol using CO<sub>2</sub> as carbon source.

Microorganism	Genes introduced for mannitol biosynthesis	Fermentation mode	Titer, g/L	Yield, [(C-mol mannitol)/(C-mol CO <sub>2</sub> )]	Maximum productivity, mg/L/h	Reference or source
<i>Synechococcus</i> sp. PCC 7002	<i>mtlD</i> from <i>E. coli</i> and <i>m1p</i> from <i>E. tenella</i>	batch	1.1	na	6.3	Jacobsen and Frigaard (2014)
<i>Synechococcus</i> sp. PCC 7002	<i>mtlD/m1p</i> fusion from <i>M. pusilla</i>	batch	0.1	na	0.004	Madsen et al. (2018)
<i>Cupriavidus necator</i> H16	<i>mtlD</i> and <i>m1p</i> from <i>E. siliculosus</i>	batch/gas fermentation	3.9	0.48*	94.2*	This study

\*average of yield and productivity monitored from 53.5 h to the 71 h time point of fermentation.

*C. necator* H16 to produce mannitol from CO<sub>2</sub> and use the flux directly from the CBB cycle via G-3-P and F-6-P intermediates. The engineered strain achieved more than 48% carbon efficiency and production of 3.9 g/L mannitol. The yield and titre is comparable to those reported for acetoin, 1,3- and 2,3-butanediols (Windhorst and Gescher, 2019; Gascoyne et al., 2021; Bommarreddy et al., 2020) in *C. necator* H16, which, however, were derived from pyruvate through the glycolysis. This is the first report of chemical bioproduction of mannitol via F-6-P intermediate using CO<sub>2</sub> as sole carbon source in *C. necator*.

### Author contributions

N.M. conceptualized the study. E.K.R.H. and N.M. designed the experiments. E.K.R.H., G.S. and N.M. carried out experiments. E.K.R.H. and N.M. wrote the manuscript. E.K.R.H., G.S., N.P.M. and N.M. reviewed and approved the manuscript.

### Acknowledgements

This work was supported by the Biotechnology and Biological Sciences Research Council (BBSRC; grant number BB/L013940/1) and the Engineering and Physical Sciences Research Council (EPSRC) under the same grant number. We thank Matthew Abbott for assistance with HPLC analysis, Josef Altenbuchner and Thierry Tonon for gifting plasmids pJH257.2, pEsM1PDH1cat and pEsM1Pase2, Rajesh Bommarreddy and Joshua Gascoyne for assistance with fermentation and data analysis, and all members of the SBRC who helped in carrying out this research.

### Appendix A. Supplementary data

Supplementary data to this article can be found online at <https://doi.org/10.1016/j.ymben.2022.02.003>.

### References

- Alagesan, S., et al., 2018a. Functional genetic elements for controlling gene expression in *Cupriavidus necator* H16. *Appl. Environ. Microbiol.* 84.
- Alagesan, S., Minton, N.P., Malys, N., 2018b. <sup>13</sup>C-assisted metabolic flux analysis to investigate heterotrophic and mixotrophic metabolism in *Cupriavidus necator* H16. *Metabolomics* 14, 1–10.
- Austubel, F.M., et al., 2003. *Current Protocols in Molecular Biology*. John Wiley & Sons.
- Bäumchen, C., Bringer-Meyer, S., 2007. Expression of *glfZ<sub>m</sub>* increases D-mannitol formation in whole cell biotransformation with resting cells of *Corynebacterium glutamicum*. *Appl. Microbiol. Biotechnol.* 76, 545–552.
- Bi, C., et al., 2013. Development of a broad-host synthetic biology toolbox for *Ralstonia eutropha* and its application to engineering hydrocarbon biofuel production. *Microb. Cell Factories* 12, 107.
- Bommarreddy, R.R., et al., 2020. A sustainable chemicals manufacturing paradigm using CO<sub>2</sub> and renewable H<sub>2</sub>. *iScience* 23, 101218.
- Bonin, P., et al., 2015. Molecular and biochemical characterization of mannitol-1-phosphate dehydrogenase from the model brown alga *Ectocarpus* sp. *Phytochemistry* 117, 509–520.
- Bushuyev, O.S., et al., 2018. What should we make with CO<sub>2</sub> and how can we make it? *Joule* 2, 825–832.
- Claassens, N.J., Sousa, D.Z., Dos Santos, V.A.M., de Vos, W.M., van der Oost, J., 2016. Harnessing the power of microbial autotrophy. *Nat. Rev. Microbiol.* 14, 692–706.
- Crépin, L., Lombard, E., Guillouet, S.E., 2016. Metabolic engineering of *Cupriavidus necator* for heterotrophic and autotrophic alka(e)ne production. *Metab. Eng.* 37, 92–101.
- Dai, Y., Meng, Q., Mu, W., Zhang, T., 2017. Recent advances in the applications and biotechnological production of mannitol. *J. Funct. Foods* 36, 404–409.
- E4tech (UK) Ltd for LBNNet, 2017. UK Top Bio-Based Chemicals Opportunities.
- Gascoyne, J.L., Bommarreddy, R.R., Heeb, S., Malys, N., 2021. Engineering *Cupriavidus necator* H16 for the Autotrophic Production of (R)-1,3-butanediol. *Metabolic Engineering*.
- Ghoreishi, S., Shahrestani, R.G., 2009. Subcritical water extraction of mannitol from olive leaves. *J. Food Eng.* 93, 474–481.
- Ghoreishi, S., Sharifi, S., 2001. Modeling of supercritical extraction of mannitol from plane tree leaf. *J. Pharmaceut. Biomed. Anal.* 24, 1037–1048.
- Grenz, S., et al., 2019. Exploiting *Hydrogenophaga pseudoflava* for aerobic syngas-based production of chemicals. *Metab. Eng.* 55, 220–230.
- Groissillier, A., et al., 2014. Mannitol metabolism in brown algae involves a new phosphatase family. *J. Exp. Bot.* 65, 559–570.
- Hanahan, D., 1983. Studies on transformation of *Escherichia coli* with plasmids. *J. Mol. Biol.* 166, 557–580.
- Hanko, E.K., Minton, N.P., Malys, N., 2018. A transcription factor-based biosensor for detection of itaconic acid. *ACS Synth. Biol.* 7, 1436–1446.
- Hoffmann, J., Altenbuchner, J., 2015. Functional characterization of the mannitol promoter of *Pseudomonas fluorescens* DSM 50106 and its application for a mannitol-inducible expression system for *Pseudomonas putida* KT2440. *PLoS One* 10, e0133248.
- Iwamoto, K., Kawanobe, H., Ikawa, T., Shiraiwa, Y., 2003. Characterization of salt-regulated mannitol-1-phosphate dehydrogenase in the red alga *Caloglossa continua*. *Plant Physiol.* 133, 893–900.
- Jacobsen, J.H., Frigaard, N.-U., 2014. Engineering of photosynthetic mannitol biosynthesis from CO<sub>2</sub> in a cyanobacterium. *Metab. Eng.* 21, 60–70.
- Ješić, D., Jurković, D.L., Pohar, A., Suhadolnik, L., Likozar, B., 2021. Engineering photocatalytic and photoelectrocatalytic CO<sub>2</sub> reduction reactions: mechanisms, intrinsic kinetics, mass transfer resistances, reactors and multi-scale modelling simulations. *Chem. Eng. J.* 407, 126799.
- Jiang, W., et al., 2021. Metabolic engineering strategies to enable microbial utilization of C1 feedstocks. *Nat. Chem. Biol.* 17, 845–855.
- Johnson, A.O., Gonzalez-Villanueva, M., Tee, K.L., Wong, T.S., 2018. An engineered constitutive promoter set with broad activity range for *Cupriavidus necator* H16. *ACS Synth. Biol.* 7, 1918–1928.
- Kamkeng, A.D., Wang, M., Hu, J., Du, W., Qian, F., 2021. Transformation technologies for CO<sub>2</sub> utilisation: current status, challenges and future prospects. *Chem. Eng. J.* 409, 128138.
- Kaup, B., Bringer-Meyer, S., Sahm, H., 2005. D-Mannitol formation from D-glucose in a whole-cell biotransformation with recombinant *Escherichia coli*. *Appl. Microbiol. Biotechnol.* 69, 397–403.
- Kondratenko, E.V., Mul, G., Baltrusaitis, J., Larrazábal, G.O., Pérez-Ramírez, J., 2013. Status and perspectives of CO<sub>2</sub> conversion into fuels and chemicals by catalytic, photocatalytic and electrocatalytic processes. *Energy Environ. Sci.* 6, 3112–3135.
- Krieg, T., Sydow, A., Faust, S., Huth, I., Holtmann, D., 2018. CO<sub>2</sub> to terpenes: autotrophic and electroautotrophic α-humulene production with *Cupriavidus necator*. *Angew. Chem. Int. Ed.* 57, 1879–1882.
- Kung, C., Martinac, B., Sukharev, S., 2010. Mechanosensitive channels in microbes. *Annu. Rev. Microbiol.* 64, 313–329.
- Lee, M.E., Aswani, A., Han, A.S., Tomlin, C.J., Dueber, J.E., 2013. Expression-level optimization of a multi-enzyme pathway in the absence of a high-throughput assay. *Nucleic Acids Res.* 41, 10668–10678.
- Lenz, O., Friedrich, B., 1998. A novel multicomponent regulatory system mediates H<sub>2</sub> sensing in *Alcaligenes eutrophus*. *Proc. Natl. Acad. Sci. Unit. States Am.* 95, 12474–12479.
- Lenz, O., Schwartz, E., Dervede, J., Eitingner, M., Friedrich, B., 1994. The *Alcaligenes eutrophus* H16 *hoxX* gene participates in hydrogenase regulation. *J. Bacteriol.* 176, 4385–4393.
- Löwe, H., Beentjes, M., Pflüger-Grau, K., Kremling, A., 2021. Trehalose production by *Cupriavidus necator* from CO<sub>2</sub> and hydrogen gas. *Bioresour. Technol.* 319, 124169.
- Madsen, M.A., Semerdzhiev, S., Amtmann, A., Tonon, T., 2018. Engineering mannitol biosynthesis in *Escherichia coli* and *Synechococcus* sp. PCC 7002 using a green algal fusion protein. *ACS Synth. Biol.* 7, 2833–2840.
- Marc, J., et al., 2017. Over expression of GroESL in *Cupriavidus necator* for heterotrophic and autotrophic isopropanol production. *Metab. Eng.* 42, 74–84.
- Milledge, J.J., Nielsen, B.V., Maneein, S., Harvey, P.J., 2019. A brief review of anaerobic digestion of algae for bioenergy. *Energy* 12, 1166.
- Müller, J., et al., 2013. Engineering of *Ralstonia eutropha* H16 for autotrophic and heterotrophic production of methyl ketones. *Appl. Environ. Microbiol.* 79, 4433–4439.
- Nangle, S.N., et al., 2020. Valorization of CO<sub>2</sub> through lithoautotrophic production of sustainable chemicals in *Cupriavidus necator*. *Metab. Eng.* 62, 207–220.
- Neves, A.R., et al., 2000. Metabolic characterization of *Lactococcus lactis* deficient in lactate dehydrogenase using *in vivo* <sup>13</sup>C-NMR. *Eur. J. Biochem.* 267, 3859–3868.
- Nybo, S.E., Khan, N.E., Woolston, B.M., Curtis, W.R., 2015. Metabolic engineering in chemolithoautotrophic hosts for the production of fuels and chemicals. *Metab. Eng.* 30, 105–120.
- Panich, J., Fong, B., Singer, S.W., 2021. Metabolic engineering of *Cupriavidus necator* H16 for sustainable biofuels from CO<sub>2</sub>. *Trends Biotechnol.* 39 (4), 412–424.
- Patra, F., Tomar, S., Arora, S., 2009. Technological and functional applications of low-calorie sweeteners from lactic acid bacteria. *J. Food Sci.* 74, R16–R23.
- Pavez, P., Honores, J., Millán, D., Isaacs, M., 2018. UN sustainable development goals: how can sustainable/green chemistry contribute? *Curr. Opin. Green Sustain. Chem.* 13, 154–157.
- Pinu, F.R., et al., 2018. Metabolite secretion in microorganisms: the theory of metabolic overflow put to the test. *Metabolomics* 14, 1–16.
- Ra, E.C., et al., 2020. Recycling carbon dioxide through catalytic hydrogenation: recent key developments and perspectives. *ACS Catal.* 10, 11318–11345.
- Raberg, M., Voigt, B., Hecker, M., Steinbüchel, A., 2014. A closer look on the polyhydroxybutyrate-(PHB-) negative phenotype of *Ralstonia eutropha* PHB4. *PLoS One* 9, e95907.
- Racine, F.M., Saha, B.C., 2007. Production of mannitol by *Lactobacillus intermedius* NRRL B-3693 in fed-batch and continuous cell-recycle fermentations. *Process Biochem.* 42, 1609–1613.
- Reshamwala, S.M., et al., 2014. Construction of an efficient *Escherichia coli* whole-cell biocatalyst for D-mannitol production. *J. Biosci. Bioeng.* 118, 628–631.
- Rousvoal, S., et al., 2011. Mannitol-1-phosphate dehydrogenase activity in *Ectocarpus siliculosus*, a key role for mannitol synthesis in brown algae. *Planta* 233, 261–273.
- Sambrook, J., Russell, D.W., 2001. *Molecular Cloning: a Laboratory Manual*, vol. 1. Cold Spring Harbor Laboratory Cold Spring Harbor, NY.

- Sand, M., et al., 2015. Mannitol-1-phosphate dehydrogenases/phosphatases: a family of novel bifunctional enzymes for bacterial adaptation to osmotic stress. *Environ. Microbiol.* 17, 711–719.
- Savergave, L.S., Gadre, R.V., Vaidya, B.K., Jogdand, V.V., 2013. Two-stage fermentation process for enhanced mannitol production using *Candida magnoliae* mutant R9. *Bioproc. Biosyst. Eng.* 36, 193–203.
- Schiener, P., Black, K.D., Stanley, M.S., Green, D.H., 2015. The seasonal variation in the chemical composition of the kelp species *Laminaria digitata*, *Laminaria hyperborea*, *Saccharina latissima* and *Alaria esculenta*. *J. Appl. Phycol.* 27, 363–373.
- Schlegel, H., Gottschalk, G., Von Bartha, R., 1961a. Formation and utilization of poly- $\beta$ -hydroxybutyric acid by Knallgas bacteria (*Hydrogenomonas*). *Nature* 191, 463–465.
- Schlegel, H., Kaltwasser, H., Gottschalk, G., 1961b. Ein Submersverfahren zur Kultur wasserstoffoxydierender Bakterien: wachstumsphysiologische Untersuchungen. *Arch. Mikrobiol.* 38, 209–222.
- Schleif, R., 2000. Regulation of the L-arabinose operon of *Escherichia coli*. *Trends Genet.* 16, 559–565.
- Schmatz, D.M., Baginsky, W.F., Turner, M.J., 1989. Evidence for and characterization of a mannitol cycle in *Eimeria tenella*. *Mol. Biochem. Parasitol.* 32, 263–270.
- Simon, R., Priefer, U., Pühler, A., 1983. A broad host range mobilization system for *in vivo* genetic engineering: transposon mutagenesis in gram negative bacteria. *Nat. Biotechnol.* 1, 784–791.
- Song, S.H., Vieille, C., 2009. Recent advances in the biological production of mannitol. *Appl. Microbiol. Biotechnol.* 84, 55–62.
- Steinbüchel, A., Schlegel, H., 1991. Physiology and molecular genetics of poly ( $\beta$ -hydroxyalkanoic acid) synthesis in *Alcaligenes eutrophus*. *Mol. Microbiol.* 5, 535–542.
- Tao, H., Bausch, C., Richmond, C., Blattner, F.R., Conway, T., 1999. Functional genomics: expression analysis of *Escherichia coli* growing on minimal and rich media. *J. Bacteriol.* 181, 6425–6440.
- Trüper, H.G., Pfennig, N., 1981. In: *The Prokaryotes* 299–312. Springer.
- Wei, N., Quarterman, J., Jin, Y.-S., 2013. Marine macroalgae: an untapped resource for producing fuels and chemicals. *Trends Biotechnol.* 31, 70–77.
- Windhorst, C., Gescher, J., 2019. Efficient biochemical production of acetoin from carbon dioxide using *Cupriavidus necator* H16. *Biotechnol. Biofuels* 12, 163.
- Wisniak, J., Simon, R., 1979. Hydrogenation of glucose, fructose, and their mixtures. *Ind. Eng. Chem. Prod. Res. Dev.* 18, 50–57.
- Wisselink, H., Weusthuis, R., Eggink, G., Hugenholtz, J., Grobden, G., 2002. Mannitol production by lactic acid bacteria: a review. *Int. Dairy J.* 12, 151–161.
- Ye, R.-P., et al., 2019. CO<sub>2</sub> hydrogenation to high-value products via heterogeneous catalysis. *Nat. Commun.* 10, 1–15.
- Yunus, I.S., et al., 2018. Synthetic metabolic pathways for photobiological conversion of CO<sub>2</sub> into hydrocarbon fuel. *Metab. Eng.* 49, 201–211.
- Zelin, J., et al., 2019. Selective aqueous-phase hydrogenation of D-fructose into D-mannitol using a highly efficient and reusable Cu-Ni/SiO<sub>2</sub> catalyst. *Chem. Eng. Sci.* 206, 315–326.